

←

TRAPPING EFFECT ON THE RESOLUTION OF Ge(Li) DETECTORS

L. Venturini and A. A. Suarez

PUBLICAÇÃO IPEN 34
IPEN - Pub - 34

SETEMBRO/1981

CONSELHO DELIBERATIVO

MEMBROS

Prof. Dr. Luiz Cintra do Prado – Presidente
Dr. Edgardo Azevedo Soares Júnior – Vice-Presidente

CONSELHEIROS

Dr. Hécio Modesto da Costa
Dr. Ivano Humbert Marchesi
Prof. Dr. Waldyr Muniz Oliva
Prof. Dr. José Augusto Martins

REPRESENTANTES

Dr. Jacob Charcot Pereira Rios
Dr. Samuel Angarita Ferreira da Silva

SUPERINTENDENTE

Hernani Augusto Lopes de Amorim

TRAPPING EFFECT ON THE RESOLUTION OF Ge(Li) DETECTORS

L. Venturini and A. A. Suarez

**CENTRO DE OPERAÇÃO E UTILIZAÇÃO DO REATOR DE PESQUISAS – COURP
ÁREA DE FÍSICA NUCLEAR**

**INSTITUTO DE PESQUISAS ENERGÉTICAS E NUCLEARES
SÃO PAULO – BRASIL**

Série PUBLICAÇÃO IPEN

INIS Categories and Descriptors

E41

LI-DRIFTED GE DETECTORS: Energy resolution

RADIATION DETECTORS: Gamma detection

CRYSTAL COUNTERS: Radiation detectors

GAMMA DETECTION: Radiation detectors

COURP - AFN

Received in October 1980.

Approved for publication in June 1981.

Writing, orthography, concepts and final revision are of exclusive responsibility of the Authors.

TRAPPING EFFECT ON THE RESOLUTION OF Ge(Li) DETECTORS

L. Venturini and A. A. Suarez

ABSTRACT

~~This work describes~~ The energy resolution variation measurement of a Ge(Li) detector as a function of irradiation position by a collimated gamma-ray beam. ~~In addition the resolution dependence has been measured as a function of the detector applied voltage, using collimated and non-collimated gamma-ray beams.~~

The measurements indicate that in the charge collection process and at the detector operation voltage, the loss of holes predominates and the best resolution is obtained in the middle of the compensated region. The dependence of the resolution on the irradiation position can be accounted for by introducing a local ionization factor different from the usual position independent Fano factor.

INTRODUCTION

The Germanium Crystals used in the fabrication of Ge(Li) detectors present structural defects and chemical impurities in such amounts that can change the properties of pure germanium. These imperfections are not totally eliminated even by using specific crystal growing techniques ⁽¹⁾ and chemical compensation of the Ge crystal. They generally give rise to allowed energy levels at the Ge forbidden gap and can act as electron-hole recombination centers or charge carriers trapping centers. As a consequence, the number of collected charges changes, breaking down the proportionality between the amount of the collected charge and the energy absorbed in the detector. Since the energy bands are properties of the entire crystal and the imperfection centers are localized, there is a dependence of the resolution on the irradiation position.

The imperfections distribution depends on the detector fabrication process and one can expect a different resolution dependence for different detectors. Thus, when using collimated beam in measurements with Ge(Li) detectors, it becomes important to know the specific detector characteristics.

EXPERIMENTAL

The detector used was an Ortec true coaxial double-open-ended Ge(Li) detector with a crystal of 44.2 mm diameter and 47.9 mm length, and 4800 volts operating voltage. The resolution measurements were taken along the radial direction of the detector. The gamma-ray beam was collimated by an 1 mm diameter and 80 mm length lead collimator coupled to the source shield. Figure 1 shows the arrangement source-collimator for the case of the ¹⁹²Ir source. The same collimator was used with the ¹⁵²Eu source.

The coordinate system origin and the dead layer center were chosen as the center of the region where a minimum counting rate was observed. Figure 2 shows the coordinate system origin where the negative and positive radius values were assumed to be on the left and right sides, respectively.

For the measurements, the pulse shape and time constants in the amplifier were selected in order to obtain the best signal-to-noise ratio. The monopolar pulse shape was used with integration and

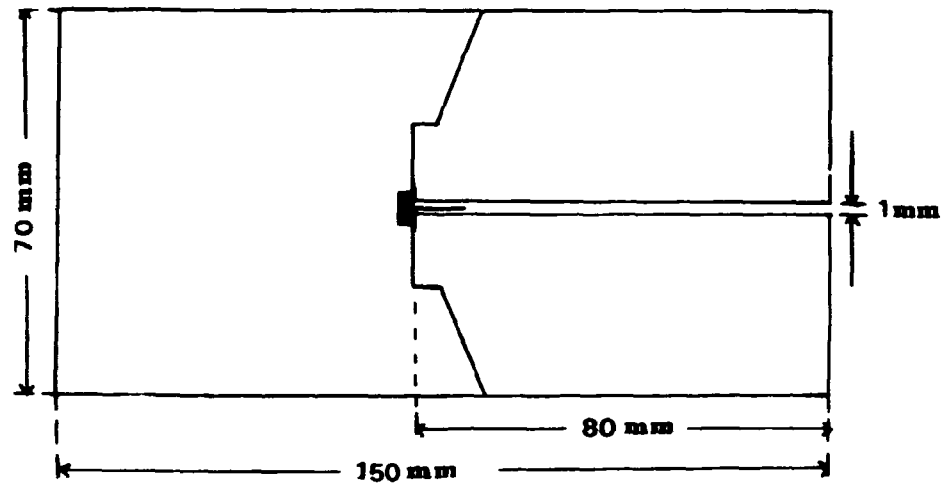


Figure 1 - Gamma-ray beam collimator with the ^{192}Ir source.

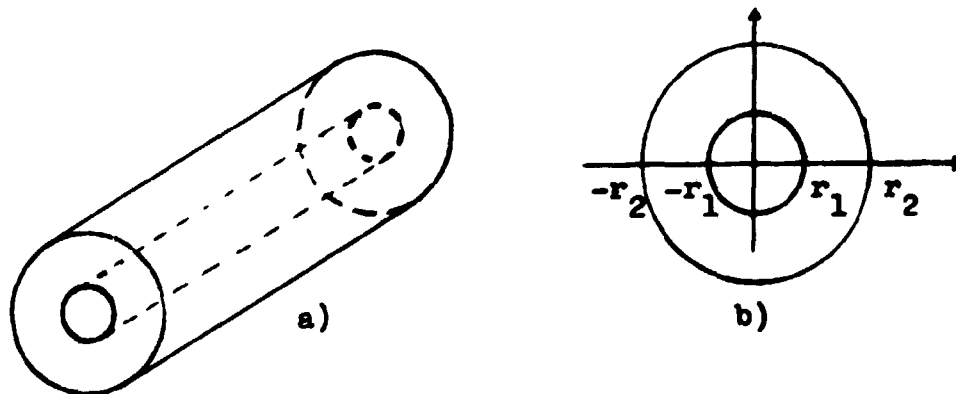


Figure 2 - a) True coaxial double-open-ended Ge(Li) crystal.
b) Coordinate system.

differentiation times equal to $2 \mu\text{sec}$. For the pole zero and base line adjustments, the counting rate was measured with collimated beam at various irradiation positions. Taking into account the statistical fluctuation, the counting rate was nearly constant for all positions except in the dead layer and in the region near the outer radius. The mean counting rate was reproduced with a non-collimated gamma-ray beam of ^{137}Cs and the pole zero and base line adjustments were taken as a mean over the entire crystal. The mean counting rate was 2200 c.p.s.

Figure 3 shows the gamma counting system.

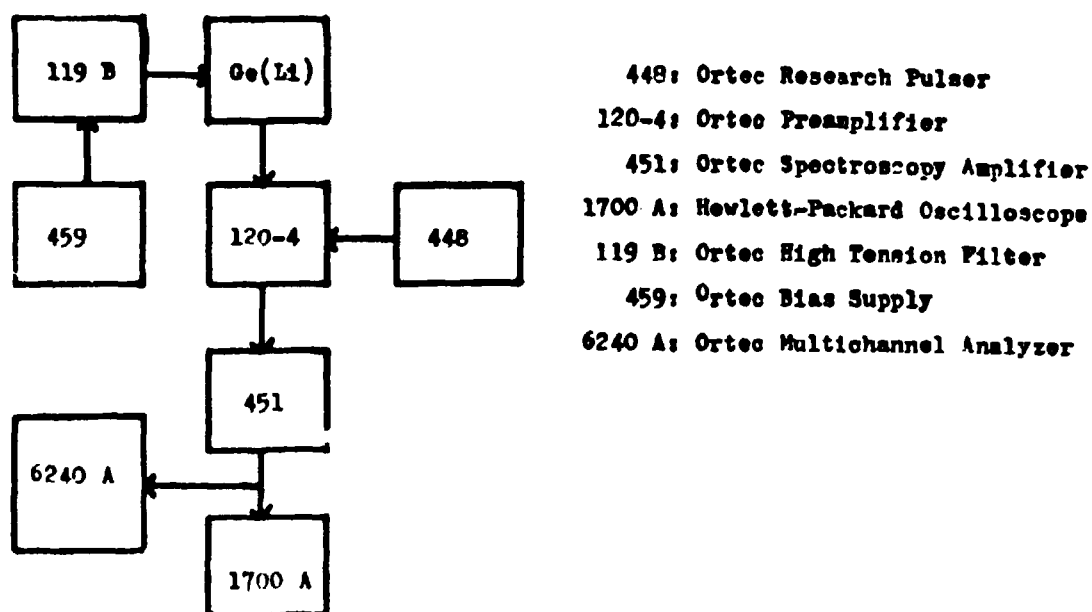


Figure 3 - Gamma-ray counting system.

The results of the resolution measurements as a function of the irradiation position as well of the detector voltage are shown in Figures 7 until 11.

DATA ANALYSIS

In the energy spectrum, the full energy peaks have Gaussian shape and the full width at half maximum (FWHM) of the peak is named resolution.

The observed resolution is the result of the electronics noise contribution and of the detector contribution. The electronics contribution was measured with the aid of a pulser. The pulser inserts, at the input of the preamplifier, a known amount of charge. Thus, any nonlinearity in the subsequent amplifier and pulse-height analysis will be the same for pulses from the detector and from the pulser. Further, the charges inserted by the pulser are not subjected to the statistical fluctuations that occur in the production and collection of electron-hole pairs in the detector.

Both, the charge collection process and the electronics noise level, have a Normal probability distribution and are independent of each other. Therefore the distribution of charge collection with electronics noise also has a Normal distribution with the variance equal to the sum of the individual variances⁽⁶⁾.

The total and the detector resolution are related by

$$(\text{FWHM})_{\text{detector}}^2 = (\text{FWHM})_{\text{total}}^2 - (\text{FWHM})_{\text{electronics}}^2$$

The fitting of the Gaussian shape to the experimental peaks was performed by a computer program⁽¹⁾. This program gives the area of the peak, the full width at half maximum and the peak position with their respective errors. The main advantage of this program is the fit of the peak tails through the use of exponentials. The Ge(Li) output function is fitted to a central Gaussian curve with smoothly joining exponentials at both sides. The background curve may be of first or second degree.

The function is represented by the expression:

$$y(x) = B + C(x-x_0) + D(x-x_0)^2 + g(x)$$

where:

$$g(x) = H \exp(-4(x-x_0)^2 \ln 2 / \Gamma^2), \quad x_0 - L_1 \leq x \leq x_0 + L_2$$

$$g(x) = H \exp(4L_1(2x - 2x_0 + L_1) \ln 2 / \Gamma^2), \quad x < x_0 - L_1$$

$$g(x) = H \exp(-4L_2(2x - 2x_0 - L_2) \ln 2 / \Gamma^2), \quad x > x_0 + L_2$$

The Gaussian has the height H , the peak position x_0 and the full width at half maximum Γ . The background function has coefficients B , C and D . Functional shapes were used for the tails in order to satisfy the smooth continuity condition between the Gaussian and the tails at the junction points $x_0 - L_1$ and $x_0 + L_2$ at the low and high energy sides respectively. The values of the eight parameters B , C , D , H , x_0 , Γ , L_1 and L_2 are determined from the least square method applied to the experimental distribution of counts c_i at the channels x_i . The solutions of the resulting normal equations are obtained by the iterative process suggested by Marquardt⁽⁵⁾.

Figure 4 shows the peak fitting for the 964 keV peak. In this figure, the crosses indicate the experimental points, the asterisks, the fitted points and the bars indicate the background.

RESULTS AND DISCUSSION

Figure 5 shows the gamma scan across a diameter of the diode. Total absorption peak counts for the 296 keV, 316 keV and 468 keV ^{192}Ir photons are plotted against beam position. The determination of the compensated region and central dead layer was performed as follows. The compensated region was taken as the distance from the first point where the counting rate in the full energy peak reaches about twice the background level to the point where the counting rate decreases with the same slope. The measurement has an uncertainty of ± 1.0 mm which corresponds to the minimum division of the collimator displacement scale. The p-core diameter was determined to be 7 mm.

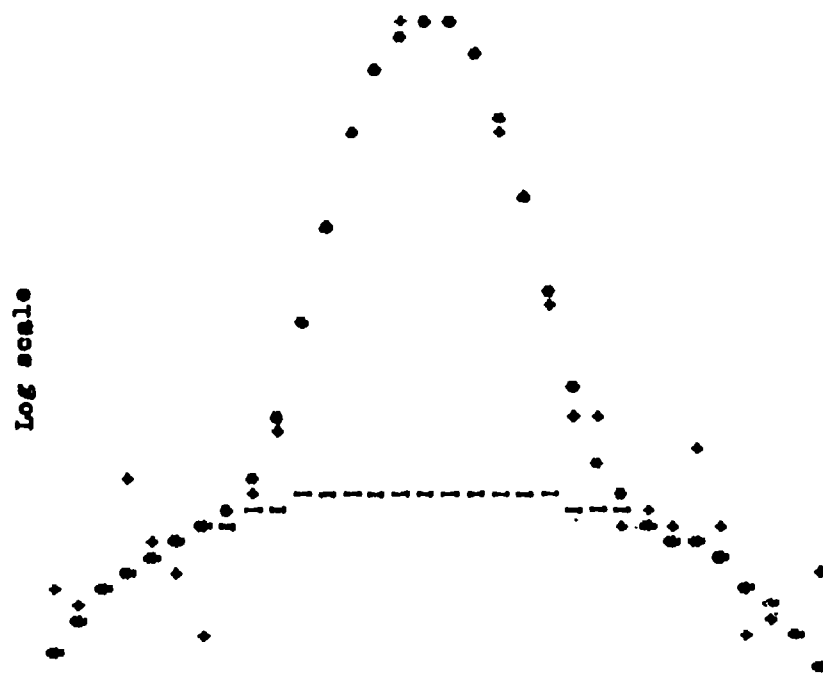


Figure 4 — Peak fit for the 964 keV peak.

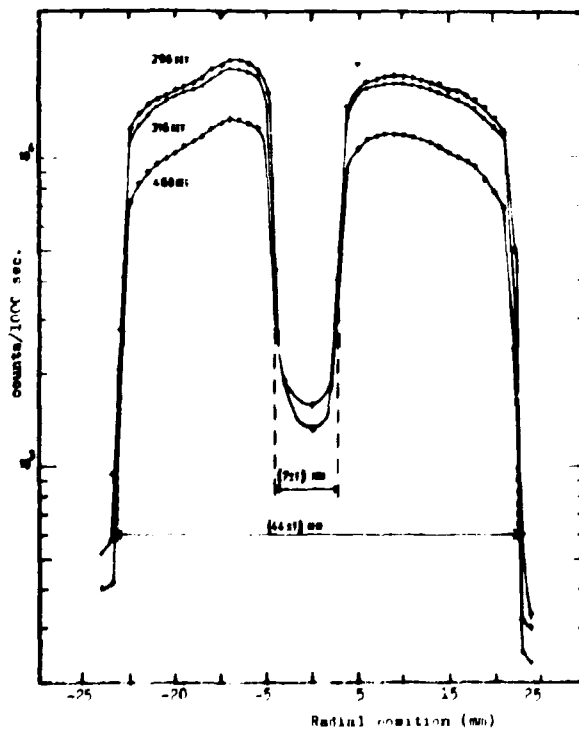


Figure 5 — Full energy peak counts as a function of the collimated gamma-ray beam incidence position.

The asymmetry of the compensated region as well the decrease of the relative peak efficiency with increasing photon energy can be seen from Figure 5. The counting rate in the full energy peak at the central dead layer falls to less than 10% of the counting rate at the compensated region.

Figure 6 shows the plot of the relative full energy peak position against beam position for the 316 keV full energy peak. In this figure, the channel number is arbitrary and the gain is 0.447 keV/channel.

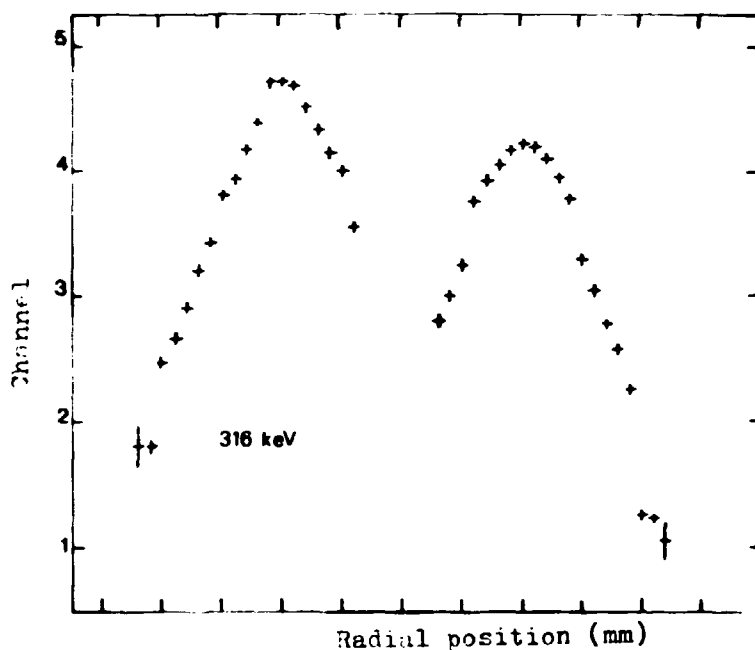


Figure 6 – Relative full energy peak position as a function of the collimated gamma-ray beam incidence position, for the 316 keV energy.

The variation of the peak position with the gamma-ray beam incidence position indicates that the charge collection is not constant across the crystal. Thus, the compensated region is not uniform.

The best charge collection efficiency is obtained for the beam incidence around the ± 10 mm radial incidence positions. The energy difference between the channels corresponding to the best and worst charge collection efficiency increases with the increasing photon energy. Table I shows the measured differences. The ^{192}Ir photons energies were taken from Gehrke⁽⁴⁾.

The loss of charge in the collection process is due to recombination and trapping. Since the counting rate was constant when the statistical fluctuations are taken into account, the recombination should not cause the peak positions shifts. Thus, the loss of charge seems to be mainly due to the trapping events. It can be concluded therefore that the trapping probability is a function of the beam incidence position as well as of the photon energy.

Figure 7 shows the Ge(Li) energy resolution (FWHM) plotted against beam incidence position. The measurements were performed for the 296 keV, 308 keV, 316 keV and 468 keV ^{192}Ir photons.

Because of the small energy difference between the 296 keV, 308 keV and 316 keV transitions, these were taken as a triplet with a single value of resolution. The measured resolution shows a small but systematic variation. The best resolution was obtained in the middle of the compensated region and the worst value was obtained for beam incidence near the outer radius. This last region is the one where the peak position indicates the greatest loss of charge during the charge collection process. The results are in agreement since the greater loss of charge results in greater statistical fluctuation in the amount of collected charge leading to worse resolution.

Table I

Energies Difference Between the Channels Corresponding to the Best and Worst Charges Collection Efficiency.

photon energy (keV)	energy difference (keV)
295.949	1.45 (0.010)
308.445	1.543 (0.010)
316.494	1.557 (0.010)
468.062	2.219 (0.010)

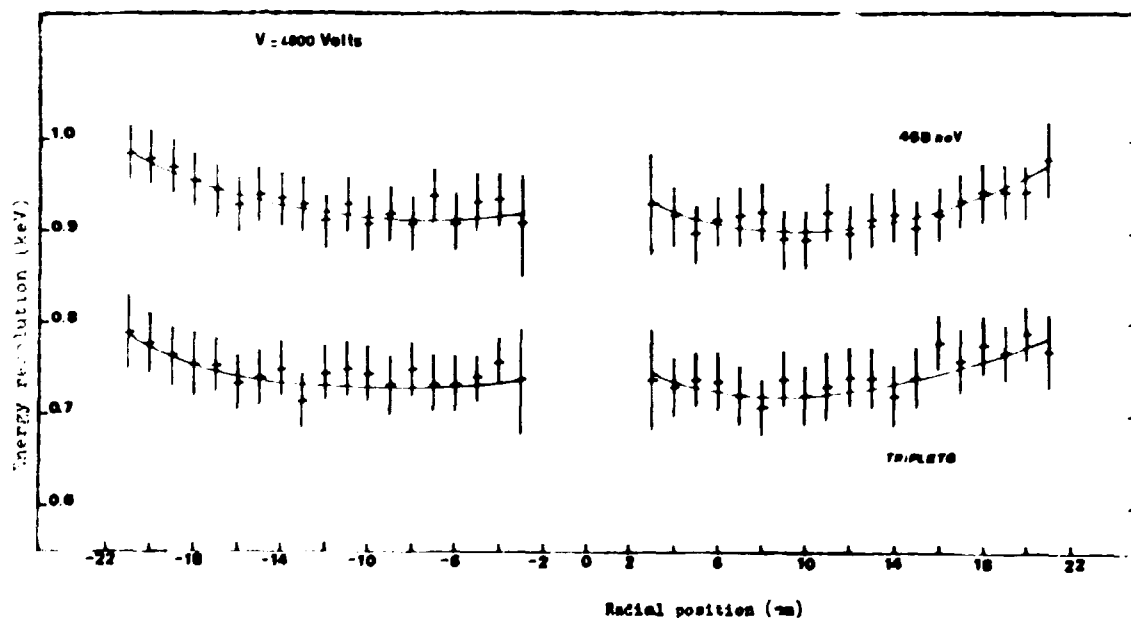


Figure 7 — Detector energy resolution as a function of the collimated gamma-ray beam incidence position.

Figure 8 shows the detector energy resolution, for the right side of the crystal, as a function of the beam incidence position. The applied voltage to the detector during the measurements were 2000, 3000 and 4800 volts. It can be seen that the resolution improves when the applied voltage increases.

From Figure 9 it can be noted that there is an increase in the charge collection efficiency with the increase of the detector voltage. In this figure, the gain is 0,494 keV/channel.

At 2000 volts, the charge collection efficiency and the detector energy resolution are better for irradiation near the outradius than for irradiation near the central dead layer. At 4800 volts, the measurements give the opposite result. Further, at 2000 volts, the best charge collection efficiency is attained for beam incidence around the 13 mm radial coordinate.

To explain this result it is necessary to consider the trajectory of the charges in the detector. The produced charges travel in the radial direction, the electrons being collected at the outer electrode and the holes at the inner electrode. When the applied voltage decreases, the trapping probability increases, but this probability decreases when the distance between the electron-hole pair and the respective collector electrodes decreases. When the irradiation occurs near the outer electrode, only holes travel through the crystal to be collected. When the irradiation occurs near the inner electrode, only electrons travel through the crystal to be collected. The worst resolution value obtained when the irradiation occurs near the inner electrode, at 2000 volts applied voltage, indicates that at this voltage loss of electrons predominates. As a consequence, the best charge collection efficiency is obtained for the beam incidence around the 13 mm radial coordinate, it means, nearer the electron collector electrode.

At 4800 volts, the worse resolution is obtained for beam incidence position near the outer radius. Thus, at the detector operation voltage, loss of holes predominates during the charge collection process.

In Figure 10 the detector energy resolution has been plotted against the detector voltage. The measurements were performed for the 964 keV ^{152}Eu photons and at the 7 mm and 17 mm beam incidence positions. Figures 8 and 10 show similar final result. The 964 keV ^{152}Eu photons have about 32 mm mean-free-path in germanium and since the crystal length is 47.9 mm one can conclude that, during the charge collection process, loss of holes predominates in the entire crystal, at the detector operation voltage.

Figure 11 shows the detector energy resolution plotted against the detector voltage. The measurements were performed for a non-collimated gamma-ray beam of ^{133}Ba . The resolution improves until the applied voltage reaches 4400 volts. Above this value it tends to be constant. The statistical fluctuation in the amount of collected charges produced in the entire crystal decreases with the increasing of the detector voltage because the mean trapping probability in the whole detector also decreases.

Above 4400 volts, the increase of the applied electrical field is no longer enough to increase significantly the charge carriers mobilities. Thus, the trapping probability can not be reduced enough to decrease the statistical fluctuation significantly. Thus, the resolution of the detector as a whole tends to reach a constant value.

From Figures 7 and 11 one can see that the detector energy resolution is better for the 468 keV collimated gamma-ray beam than for the 356 keV non-collimated gamma-ray beam. This result can be explained on the basis of the non-uniformity of the compensated region. The statistical fluctuation in the amount of collected charge produced in the whole detector will be greater than for the charges produced in only a fraction of the crystal volume. Thus, the resolution is better when collimated beam is used.

For our detector we also performed a calculation of the Fano factor⁽³⁾ by considering that the

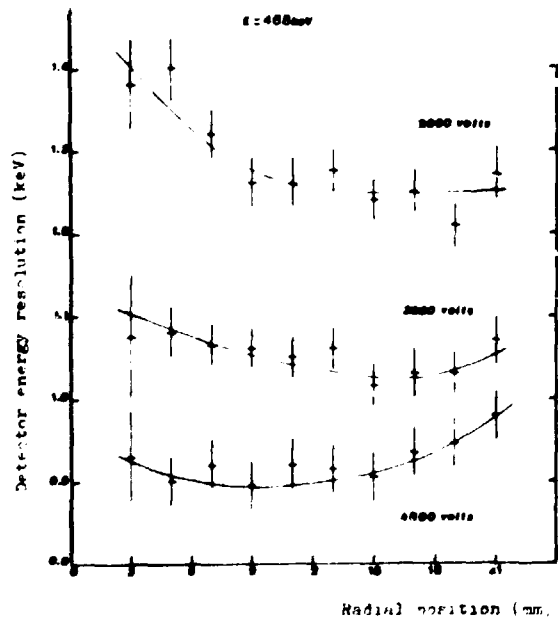


Figure 8 - Detector energy resolution as a function of the collimated gamma-ray beam incidence position for different applied voltages.

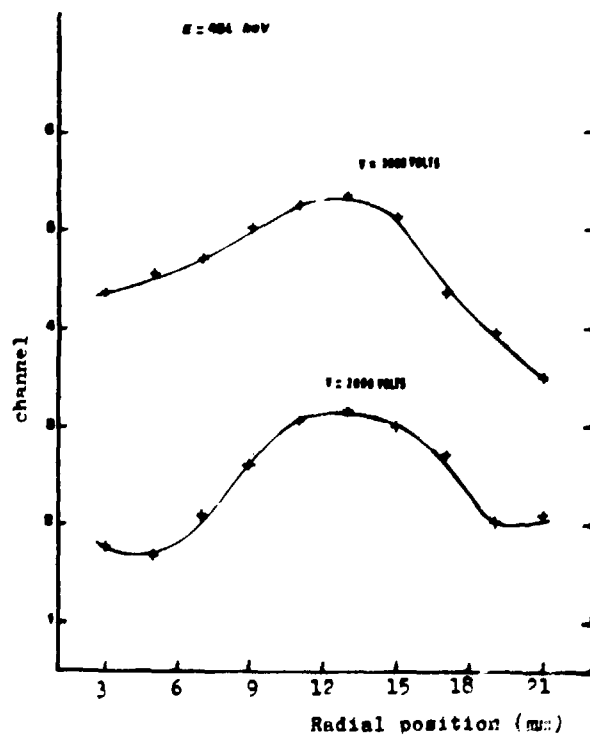


Figure 9 - Relative full energy peak position as a function of the collimated gamma-ray beam incidence position.

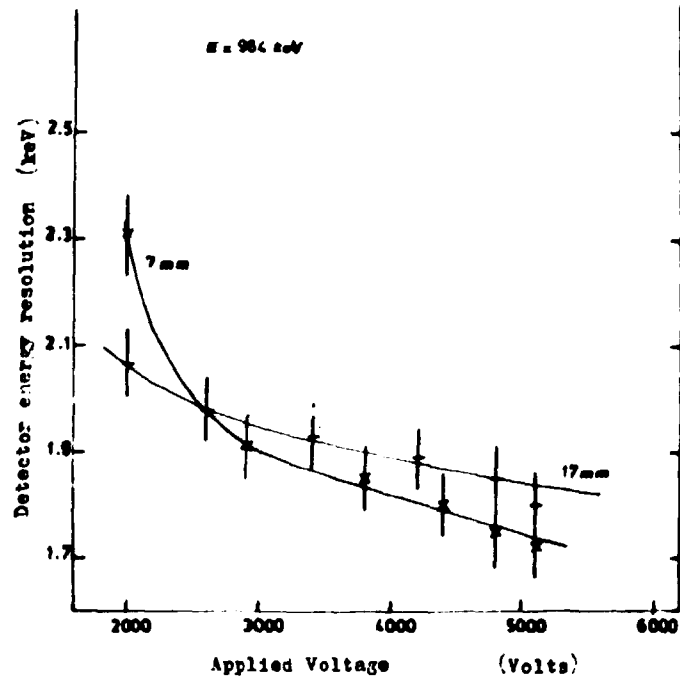


Figure 10 - Detector energy resolution (FWHM) as a function of the applied voltage.

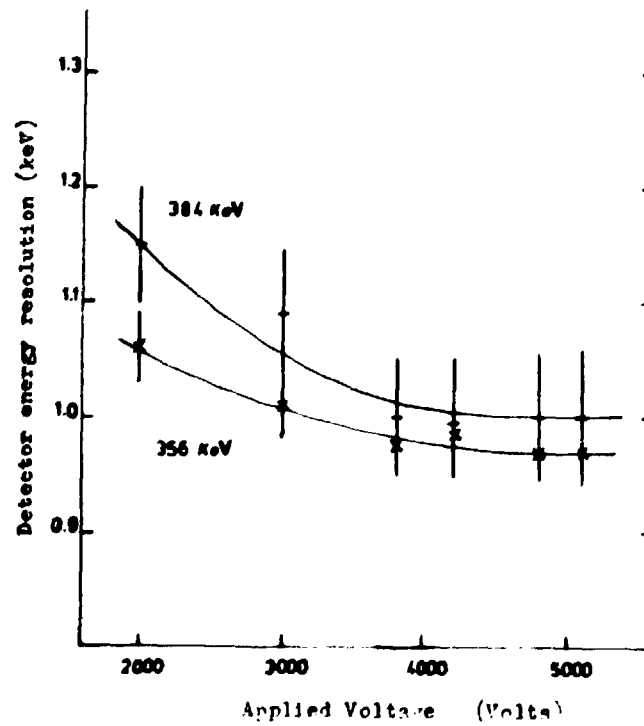


Figure 11 - Detector energy resolution (FWHM) as a function of the applied voltage for a noncollimated ^{133}Ba gamma-ray beam.

theoretical and experimental resolutions have same value. From the Gaussian shape of the peaks and considering only the detector contribution to the resolution, the full width at half maximum is given by $\text{FWHM} = \sigma(8 \ln 2)^{1/2}$. Here σ is the standard deviation of the number of electron-hole pairs produced by photons whose energy corresponds to the peak in consideration.

In terms of energy the FWHM, or the resolution, is given by $\Gamma = (8 w E F \ln 2)^{1/2}$, where:

w = mean energy needed to form a electron-hole pair⁽²⁾,

E = photon energy (keV).

F = Fano factor,

Γ = energy resolution FWHM (keV).

If $\Gamma_{\text{experimental}} = \Gamma_{\text{theoretical}}$, we have:

$$8 w E F \ln 2 = \Gamma_{\text{total}}^2 - \Gamma_{\text{pulser}}^2 = \Gamma_{\text{detector}}^2$$

$$F = \Gamma_{\text{detector}}^2 / (8 w E \ln 2)$$

By the theory⁽³⁾ the Fano factor relates the experimental variance and the variance given by Poisson distribution. This factor is introduced in order to take into account the fact that the process of loss of energy in the crystal are not independent. Thus, it should be energy and ionization position independent. The present calculation however shows that F depends on the photon energy as well on the irradiation position as shown in Figure 12. We therefore replaced the F factor by a factor F' which includes the dependence of the resolution on the irradiation position.

For the right side of the detector one finds two regions where F' presents a linear energy dependence with the same mean coefficients:

$$F' = \bar{a}_0 + \bar{a}_1 \cdot E \quad 3 \text{ mm} < r < 16 \text{ mm}$$

$$F' = \bar{a}_0 + \bar{a}_1 \cdot E \quad 16 \text{ mm} < r < 21 \text{ mm}$$

where

$$\bar{a}_0 = 0.050 \text{ (0.005)}$$

$$\bar{a}_1 = 0.000140 \text{ (0.000008) keV}^{-1}$$

$$\bar{a}_1 = 0.000199 \text{ (0.000022) keV}^{-1}$$

In the linear relations, \bar{a}_0 is a constant for the whole right side of the crystal. We believe that \bar{a}_0 is the usual position independent Fano factor. The value of \bar{a}_0 agrees with experimental values obtained by Zulliger⁽⁹⁾ and Sher and Keery⁽⁸⁾.

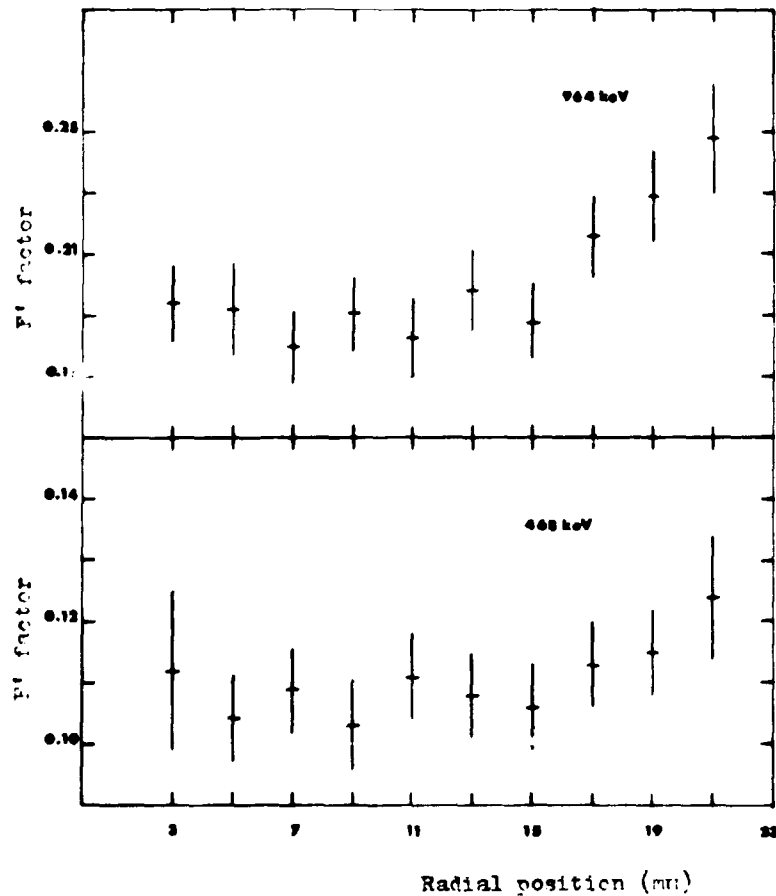


Figure 12 — F' factor as a function of the irradiation position.

The $a_1.E$ term represents the energy and irradiation position dependence of F' . We already pointed out that the trapping probability seems to be a function of the energy and of the irradiation position. It is possible that the a_1 coefficient is related with the trapping centers distribution which can vary with the crystal. We also believe that the $a_1.E$ term takes into account the Compton scattering of photons in the detector. The Compton Effect results in the increase of the ionization volume thereby increasing the number of trapping centers which can attract the charge carriers and increase the trapping probability. The F' factor appears to be a linear combination of the usual position independent Fano factor and a local ionization factor.

CONCLUDING REMARKS

In the detector used, the resolution was observed to vary with the photon energy and the beam incidence position. The best energy resolution was obtained in the middle of the compensated region. Since the resolution seems to depend on the distance between the ionization volume and the collector electrodes, one can expect that a crystal with a lower diameter will present better resolution although with worse relative peak efficiency. Further, the best resolution irradiation position may not be the best relative peak efficiency irradiation position.

The detector energy resolution is better when only a limited region of the crystal is irradiated. It means, the best geometry for a good energy resolution is that which uses collimated beams.

The experimental resolution can be estimated by using the F' factor in the theoretical energy resolution expression. The dependence of the resolution on the ionization volume is accounted for by introducing the F' factor different from the usual position independent Fano factor.

ACKNOWLEDGMENTS

The authors thank to M. Sc. C. R. S. Stopa and Dr. B. R. S. Pecequillo for their help in the solution of electronics problems and are indebted to Dr. G. Vandenput who provided the computer program used in the present work.

RESUMO

Estudo
Neste trabalho foi estudada a variação da resolução de um detector Ge(Li) como função da posição de incidência de um feixe gama colimado no cristal. Estudou-se também a variação da resolução como função da tensão aplicada ao detector usando-se feixes gama colimados e não colimados.

Os resultados mostram que, na tensão de operação do detector, durante o processo de coleção de cargas, ocorre perda preferencial de buracos e a melhor resolução é obtida no centro da região compensada. A resolução em energia do detector é função de um fator F' , dependente da energia e de posição de irradiação, diferente do fator de Fano considerado constante. *(Autogr.)*

REFERENCES*

1. "ANALYSIS". A routine Fortran IV program available in IPEN Computer Center.
2. ANTMAN, S. O. W.; LANDIS, D. A.; PEHL, R. H. Measurements of the Fano factor and the energy per hole-electron pair in germanium. *Nucl. Instr. Meth.*, 40:272-6, 1966.
3. FANO, U. Ionization yield of radiations. II. The fluctuations of the number of ions. *Phys. Rev.*, 72(1):26-9, 1947.
4. GEHRKE, R. J. The decay of ^{192}Ir . *Nucl. Phys.*, A204:26-32, 1973.
5. MARQUANDT, D. W. An algorithm for least-squares estimation of non-linear parameters. *J. Sec. ind. appl. Math.*, 11(2):431-41, 1963.
6. NICHOLSON, P. W. *Nuclear Electronics*. N. York, John Wiley, 1974.
7. RHODES, R. G. *Imperfections and active centers in semiconductors*. N. York, Pergamon Press, 1964. (International Series of Monographs on Semiconductors, vol. 6).
8. SHER, A. H. & KEERY, W. J. Variation of the effective Fano factor in a Ge(Li) detector. *IEEE Trans. Nucl. Sci.*, NS-17(1):39-43, 1970.
9. ZULLIGER, H. R. Fano factor fact and falacy. *IEEE Trans. Nucl. Sci.*, NS-17(3):187-92, 1970.

(*) Bibliographic references related to documents belonging to IPEN Library were revised according with NB-66 Associação Brasileira de Normas Técnicas.

INSTITUTO DE PESQUISAS ENERGÉTICAS E NUCLEARES
Caixa Postal, 11 049 – Pinheiros
CEP 05506
01000 – São Paulo – SP

Telefone: 211-6011
Endereço Telegráfico – IPENUCLEAR
Telex – (011) 23592 - IPEN - BR